12. DEEP SPACE PLASMA MEASUREMENTS*

12.1. Introduction

This chapter describes experimental methods used for the study of plasma in extraterrestrial space by means of instruments carried on earth satellites and space probes. The techniques to be described were developed primarily for observations within the interplanetary medium (the solar wind) (cf. review by Hundhausen[1]) but have also been used for the study of plasma within the magnetosheath and more recently within the magnetotail and the outer magnetosphere[2] (also see review by Gringauz[3]). (Figure 1 illustrates the division of space into distinct regions on the basis of plasma properties and identifies the nomenclature.) This chapter deals only with measurements beyond the plasmasphere. Not included are methods used primarily for observations of ionospheric plasma. The emphasis is on the physical principles underlying the instrumentation and on the methods for analyzing the observations. The specialized technological problems raised by spacecraft operation (such as power and weight limitation, reliability, thermal control, and compatibility with other spacecraft systems) belong to engineering rather than physics and will not be treated here.

12.1.1. Microscopic Character of the Instruments

Space plasma differs in many respects from laboratory plasma and requires correspondingly different measurement techniques. The most obvious is a difference of scale. Table I summarizes some of the properties of plasma observed in various regions of space. Of the various characteristic lengths that can be defined in a plasma, the shortest in practically all explored regions of extraterrestrial space is the Debye length, which nonetheless has a value of the order of or greater than 10 meters. On

[1] A. J. Hundhausen, *Space Sci. Rev.* **8,** 690 (1968).

[2] S. J. Bame, *in* "Earth's Particles and Fields" (B. M. McCormac, ed.), p. 359. Reinhold, New York, 1968.

[3] K. I. Gringauz, *Rev. Geophys.* **7,** 339 (1969).

* Part 12 by Vytenis M. Vasyliunas.

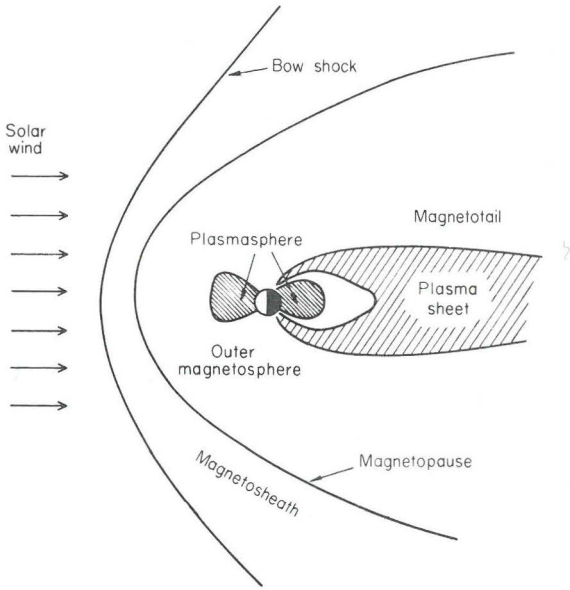

FIG. 1. Sketch of the principal plasma regions found in outer space within $\sim 10^5$ km of the earth. The view is in the noon–midnight meridian plane. The "plasmasphere" is a region of very dense ($\gtrsim 10^3$ particles/cm^3) cold plasma that can be considered an extension of the ionosphere. The earth's magnetic field is effectively confined to a region contained within a surface called the magnetopause. The part of this region lying on the dark side of the earth is usually called the magnetotail or magnetospheric tail and contains a central region of enhanced particle fluxes, the plasma sheet. The magnetopause acts as an obstacle to solar wind flow, which undergoes a sharp shocklike transition (the bow shock) upstream of it. The region between the bow shock and the magnetopause is termed the magnetosheath (an older, now obsolete, term is "transition region"). [For a more detailed description, see, e.g. S. J. Bame, *in* "Earth's Particles and Fields" (B. M. McCormac, ed.), p. 359. Reinhold, New York, 1968, and K. I. Gringauz, *Rev. Geophys.* **7**, 339 (1969), and references therein.]

the other hand, the largest plasma detectors flown have dimensions not exceeding 10 cm and are carried by satellites usually no more than several meters in size (although many satellites have long thin booms that may reach 20–30 meters). Hence the length scale of the instrument is much shorter than any of the characteristic length scales of the plasma, and on this scale the plasma is expected to appear as merely an assemblage of non-interacting charged particles, without the collective behavior generally implied by the word *plasma*. Satellite-borne plasma detectors, accordingly, are not plasma instruments in the sense that, e.g., Langmuir probes are; they are simply devices for the detection and analysis of charged particle beams.

TABLE I. Typical Orders of Magnitude of Plasma Parameters in Various Regions of Outer Space

	Solar wind	Magneto-sheath	Outer magnetosphere and plasma sheet
Particle density ($1/cm^3$)	10	20	1
Temperature (eV)	10	10^2	10^3
Bulk flow speed (km/sec)	4×10^2	2×10^2	10
Magnetic field (gauss)	5×10^{-5}	10^{-4}	2×10^{-4}
Total particle flux ($1/cm^2/sec$)			
protons	10^8	10^8	4×10^7
electrons	10^9	5×10^9	2×10^9
Length scales, km			
Debye length	10^{-2}	2×10^{-2}	3×10^{-1}
electron gyroradius[a]	2	3	5
proton gyroradius[a]	3×10^3	5×10^3	10^4
scale sizes of typical structures	10^6–10^8	10–10^4	10^4–10^5
mean free path[b]	2×10^7	10^9	2×10^{12}

[a] Based on thermal speed.

[b] For proton–proton Coulomb collisions.

12.1.2. The Problem of Spacecraft–Plasma Interaction

Two further properties of extraterrestrial plasma should be noted from Table I: (a) typical particle energies range from about 10 eV to several kiloelectron volts; (b) the total electron flux generally considerably exceeds the total positive ion flux. From the latter fact one might expect that a spacecraft immersed in such a plasma would quickly acquire a negative charge sufficient to repel most of the electrons in order to have no net current to the spacecraft. This would imply a negative spacecraft potential with respect to the plasma of the order of the mean electron energy per unit charge, large enough to affect seriously any plasma measurements being made. However, several effects exist that may prevent the buildup of such large potentials. The most important arises from the fact that the spacecraft is continually exposed to sunlight; thus photoelectrons are produced at the surface of the spacecraft, with energies of a few electron volts, and their total flux is believed to be of the order of 10^{-8} A/cm^2 ($\sim 10^{11}$ electrons/cm^2/sec),[4] comparable to or larger than the total plasma electron flux. Furthermore, electrons of several hundred electron volts energy striking a metal surface produce secondary electrons, again with energies of a few electron volts; the average number of secondaries

[4] H. E. Hinteregger, K. R. Damon, and L. A. Hall, *J. Geophys. Res.* **64**, 961 (1959).

per incident electron may exceed unity,[5] leading to a net positive current from electron bombardment. The possibility thus exists that the condition of zero net current to the spacecraft is achieved, not by repelling the plasma electron flux, but by balancing it with a large outgoing photoelectron (and perhaps secondary electron) flux; the spacecraft potential then might be only of the order of a few volts and would not appreciably affect the typical plasma measurements at energies of tens of electron volts and higher. To the author's knowledge, a detailed study of the spacecraft-plasma interaction, taking into account the important factors of energetic plasma particle flux, photoelectron and secondary electron emission, does not exist and the aforementioned possibility has been neither justified nor disproved (existing treatments of the problem[6] deal only with low-energy ionospheric plasma and neglect photoelectron effects).

As a practical matter, in all observational work reported to date, it has been assumed that spacecraft potentials do not significantly affect any particles with energies higher than ~ 10 eV, and that fluxes of these particles detected by instruments on the spacecraft accurately represent the fluxes present in the plasma. This assumption is to some extent supported by the actual observations, which show that the plasma electron flux incident on the spacecraft is indeed much larger than the positive ion flux; furthermore, the total number density of the observed electrons is, within errors of measurement, equal to the number density of the observed positive ions,[2,7] as it should be if the measurements indicate conditions in the plasma and are not affected by the spacecraft.

12.2. Instrumentation

12.2.1. General Survey

The first observations of extraterrestrial plasma were made by Gringauz and co-workers[8] by means of very simple probes consisting of a collector plate behind a grid carrying a steady retarding potential (of the order of 10 volts in these measurements). Measurement of the current to the collector indicated the flux of positive ions (or electrons, depending on the polarity of the retarding potential) whose energies per unit charge exceeded the potential on the retarding grid. An additional grid, negatively biased with respect to the collector, was inserted between the collector and the

[5] K. G. McKay, *Advan. Electron.* **1,** 65 (1948).

[6] L. W. Parker and B. L. Murphy, *J. Geophys. Res.* **72,** 1631 (1967).

[7] M. D. Montgomery, S. J. Bame, and A. J. Hundhausen, *J. Geophys. Res.* **73,** 4999 (1968).

[8] K. I. Gringauz, V. V. Bezrukikh, V. D. Ozerov, and R. E. Rybchinskii, *Dokl. Akad. Nauk SSSR* **131,** 1301 (1960); *Sov. Phys. Dokl.* **5,** 361 (1961).

retarding grid in order to suppress emission of photoelectrons from the collector; fairly large corrections still had to be made for photoelectron emission from the suppressor grid itself. Instruments of this type have been widely used for measurements of ionospheric plasma[9]; however, they have not been successfully adapted to measure plasma of the kind found in the solar wind and will not be further discussed here.

Two types of instruments have been providing the bulk of deep space plasma observations to date. The first, the modulated-potential Faraday cup, introduced[10] and extensively used by the M.I.T. group, is in many respects similar to the retarding potential probe just discussed but uses an alternating instead of a steady retarding potential to obtain a measurement of the plasma particle energy spectrum. The second selects particles of a specified energy by requiring them to pass between two curved plates with a potential difference between them. An important improvement possible with detectors of the second type is the measurement of flux by counting individual particles rather than measuring currents electrically, thus allowing a considerable increase in sensitivity.

All these instruments can only measure the energy per charge spectrum of the particles. Since hydrogen is expected to be the dominant constituent of extraterrestrial space, it has usually been assumed that the negative particles observed were all electrons and the positive particles predominantly protons (however, significant amounts of alpha particles, which are expected to have the same bulk speed as the protons and hence twice the energy per charge, have always been found in the solar wind). An instrument capable of distinguishing individual ion species has recently been developed by combining a curved-plate analyzer with a crossed electric and magnetic field velocity selector.[11,12]

In this section the general properties of these various types of detectors will be described, in a systematic rather than historical sequence. A list of the spacecraft that have carried plasma detectors appears in Table II, together with references to available descriptions of the instruments.

12.2.2. Energy Measurement

12.2.2.1. The Modulated-Potential Faraday Cup—Basic Principles. In its simplest form the modulated-potential Faraday cup, shown schemati-

[9] W. C. Knudsen, *J. Geophys. Res.* **71,** 4669 (1966).

[10] H. S. Bridge, C. Dilworth, B. Rossi, F. Scherb, and E. F. Lyon, *J. Geophys. Res.* **65,** 3053 (1960).

[11] K. W. Ogilvie, N. McIlwraith, and T. D. Wilkerson, *Rev. Sci. Instrum.* **39,** 441 (1968).

[12] K. W. Ogilvie, R. I. Kittredge, and T. D. Wilkerson, *Rev. Sci. Instrum.* **39,** 459 (1968).

TABLE II. Deep Space Plasma Experiments, 1959–1968[a]

Spacecraft	Year of launch	Type of detector[b]	Experimenters[c] and references[d]
Lunik 1	1959	RPP	Acad. Sci. U.S.S.R.[e]
Lunik 2	1959	RPP	Acad. Sci. U.S.S.R.
Lunik 3	1959	RPP	Acad. Sci. U.S.S.R.
Venus 1	1961	RPP	Acad. Sci. U.S.S.R.
Explorer 10	1961	MFC	M.I.T.[f]
Explorer 12	1961	CPA	Ames[g]
Mariner 2	1962	CPA	J.P.L.[h]
Explorer 14	1962	CPA	Ames
Mars 1	1962	RPP	Acad. Sci. U.S.S.R.
Explorer 18 (IMP 1)	1963	MFC	M.I.T.[i]
		CPA	Ames[j]
Electron 2	1964	RPP	Acad. Sci. U.S.S.R.
		CPA	Acad. Sci. U.S.S.R.[k]
Vela 2A, 2B	1964	CPA	Los Alamos[l]
OGO 1	1964	MFC	M.I.T.[m]
		CPA	Ames
Explorer 21 (IMP 2)	1964	MFC	M.I.T.
		CPA	Ames
Mariner 4	1964	MFC	M.I.T.–J.P.L.[n]
Zond 2	1964	RPP	Acad. Sci. U.S.S.R.
Explorer 28 (IMP 3)	1965	MFC	M.I.T.
		CPA	Ames
Vela 3A, 3B	1965	CPA	Los Alamos
Venus 2	1965	RPP	Acad. Sci. U.S.S.R.
Venus 3	1965	RPP	Acad. Sci. U.S.S.R.
Pioneer 6	1965	MFC	M.I.T.[o]
		CPA	Ames[p]
Luna 10	1966	RPP	Acad. Sci. U.S.S.R.
OGO 3	1966	MFC	M.I.T.
		CPA	Ames
		CPA	Iowa[q]
Explorer 33	1966	MFC	M.I.T.[r]
Pioneer 7	1966	MFC	M.I.T.
		CPA	Ames
ATS 1	1966	MFC	Rice[s]
Explorer 34 (IMP F)	1967	CPA-VS	GSFC–Maryland[t]
		CPA	Iowa
Venus 4	1967	RPP	Acad. Sci. U.S.S.R.
Mariner 5	1967	MFC	M.I.T.–J.P.L.
Explorer 35	1967	MFC	M.I.T.
Vela 4A, 4B	1967	CPA	Los Alamos[u]
Pioneer 8	1967	CPA	Ames
OGO 5	1968	CPA	Iowa
		MFC, CPA	J.P.L.

* See p. 55 for footnotes to table.

cally in Fig. 2, consists of a cylindrical metal cup open at one end with a collector plate at the other end and a minimum of four planar grids. Grid 1 is usually grounded (throughout this chapter "ground" means the potential of the skin of the spacecraft which, as discussed previously, is assumed to differ by no more than some few volts from the potential of the surrounding plasma); it and the walls of the cup, also grounded, form a closed equipotential surface around the detector and prevent any electric fields generated within the detector from penetrating outside. Grid 2 is

---

[a] Only instruments intended for the study of plasma in the outer magnetosphere and beyond are included. The list may not be complete.

[b] RPP is the retarding potential (dc) probe; MFC is the modulated Faraday cup; CPA the curved-plate analyzer; VS the velocity selector.

[c] Acad. Sci. U.S.S.R. is the Academy of Sciences of the U.S.S.R.; M.I.T. is the Massachusetts Institute of Technology; Ames is the NASA Ames Research Center; J.P.L. is the Jet Propulsion Laboratory, California Institute of Technology; Los Alamos is the Los Alamos Scientific Laboratory, University of California; Iowa is the University of Iowa; Rice is the Rice University; GSFC–Maryland is the NASA Goddard Space Flight Center and University of Maryland.

[d] Only published papers containing descriptions of instrumentation are included. Essentially identical instruments have often been flown on several spacecraft; in such cases only the first one has been referenced.

[e] K. I. Gringauz, V. V. Bezrukikh, V. D. Ozerov, and R. E. Rybchinskii, *Dokl. Akad. Nauk SSR* **131,** 1301 (1960); *Sov. Phys. Dokl.* **5,** 361 (1961).

[f] A. Bonetti, H. S. Bridge, A. J. Lazarus, B. Rossi, and F. Scherb, *J. Geophs. Res.* **68,** 4017 (1963).

[g] M. Bader, *J. Geophys. Res.* **67,** 5007 (1962).

[h] M. Neugebauer and C. W. Snyder, *J. Geophys. Res.* **71,** 4469 (1966).

[i] H. S. Bridge, A. Egidi, A. Lazarus, E. Lyon, and L. Jacobson, *Space Res.* **5,** 969 (1965).

[j] J. H. Wolfe, R. W. Silva, and M. A. Myers, *J. Geophys. Res.* **71,** 1319 (1966).

[k] S. N. Vernov, V. V. Melnikov, I. A. Savenko, and B. I. Savin, *Space Res.* **6,** 746 (1966).

[l] S. Singer, *Proc. IEEE* **53,** 1935 (1965).

[m] V. M. Vasyliunas, *J. Geophys. Res.* **73,** 2839 (1968).

[n] A. J. Lazarus, H. S. Bridge, J. M. Davis, and C. W. Snyder, *Space Res.* **7,** 1296 (1967).

[o] A. J. Lazarus, H. S. Bridge, and J. Davis, *J. Geophys. Res.* **71,** 3787 (1966).

[p] J. H. Wolfe, R. W. Silva, D. D. McKibbin, and R. H. Mason, *J. Geophys. Res.* **71,** 3329 (1966).

[q] L. A. Frank, *J. Geophys. Res.* **72,** 185 (1967).

[r] E. F. Lyon, H. S. Bridge, and J. H. Binsack, *J. Geophys. Res.* **72,** 6113 (1967).

[s] J. W. Freeman, Jr., *J. Geophys. Res.* **73,** 4151 (1968).

[t] K. W. Ogilvie, N. McIlwraith, and T. D. Wilkerson, *Rev. Sci. Instrum.* **39,** 441 (1968).

[u] M. M. Montgomery, S. J. Bame, and A. J. Hundhausen, *J. Geophys. Res.* **73,** 4999 (1968).

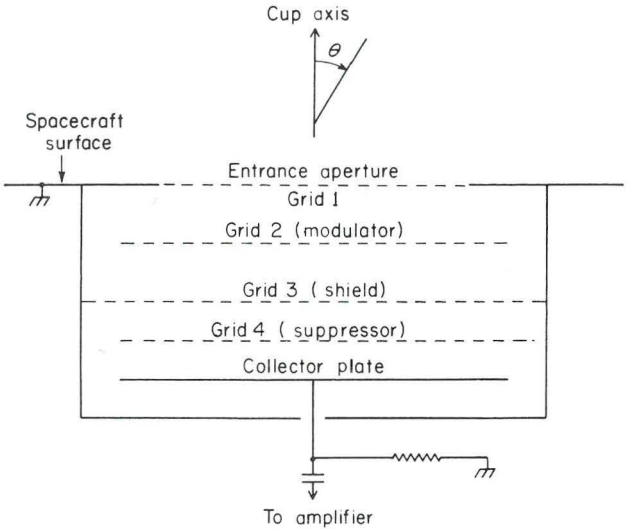

FIG. 2. Schematic diagram of the modulated-potential Faraday cup.

the modulator grid; an alternating potential, usually in the form of a square wave at a frequency of a few kilohertz, is applied to it. Grid 3, the shield grid, is grounded and prevents the modulator potential from inducing currents on the collector by direct capacitive coupling. Grid 4 is maintained at a steady negative potential (typical values range from -50 to -150 volts) and serves to suppress the emission of photoelectrons and/or secondary electrons from the collector plate.

A typical instrument may have a diameter of ~ 10 cm and a depth of ~ 5 cm. The shield grid is usually a phosphor-bronze grid with an optical transparency of $\sim 33\%$ at normal incidence; the others are $\sim 90\%$ transparent tungsten grids.

To describe the functioning of the instrument, let V_1 and V_2 be the limits of the square wave modulator potential; $V_2 > V_1$ and either $V_1 > 0$ or $V_2 < 0$, depending on whether positive or negative particles are to be measured. Consider a particle of charge q and kinetic energy E incident at an angle θ to the axis of the cup. Then if

$$E \cos^2 \theta < qV_1, \tag{12.2.1}$$

the particle is reflected by the modulator grid at all times. If

$$qV_1 < E \cos^2 \theta < qV_2, \tag{12.2.2}$$

the particle can reach the collector during the lower half of the modulation cycle (modulator potential is V_1) and is reflected by the modulator grid

during the upper half (V_2), thus producing an alternating current at the collector that is at the same frequency as the modulator potential and is 180° out of phase. Finally, if

$$qV_2 < E\cos^2\theta \tag{12.2.3}$$

(this includes particles of opposite polarity to the modulator potential), the particle can reach the collector at all times and produces only a steady current, to first approximation (corrections to this are discussed further on). (Negative particles for which $E\cos^2\theta/q < V_s$, the potential on the suppressor grid, never reach the collector regardless of the modulator potential.)

The current to the collector thus contains two components: an alternating current proportional to the flux of incident particles satisfying Eq. (12.2.2), and a steady current due to other particles. The alternating current is measured and provides information on particles within the "energy window" defined by (12.2.2). By varying the limits of the modulating potential, particles in different "energy windows" can be observed.

12.2.2.1.1. HIGHER-ORDER CORRECTIONS. The distance between adjacent grids is usually made small compared to the diameter of the cup; hence the electric fields in the center of the cup can be calculated to a good approximation by treating the grids as infinite equipotential planes. An incident charged particle with sufficient energy to reach the collector (i.e., satisfying Eq. (12.2.3)) may nevertheless be affected by the modulator: if it is incident at a nonzero angle to the cup axis, it will be laterally displaced in passing through the electric fields of the modulator by an amount ΔL that is readily shown to be

$$\Delta L = L\tan\theta\,\frac{1-(1-x)^{1/2}}{1+(1-x)^{1/2}},$$
$$x \equiv qV/E\cos^2\theta, \tag{12.2.4}$$

where V is the potential on the modulator and L is the distance between the two grounded grids surrounding the modulator (i.e., grids 1 and 3). The largest possible displacement, which occurs when either $x \to 1$ or $x \to -\infty$, has the magnitude L. If a particle reaches the collector plate near its edge, the difference between the lateral displacements at the upper and lower values of the modulator potential may be large enough so that the particle strikes the collector during one but misses it during the other, thus giving rise to an alternating current (it can be easily seen that this current is also 180° out of phase with the modulator potential). Thus the alternating current measures not only the flux of particles satisfying

Eq. (12.2.2), i.e., lying within the nominal energy window of the detector, but also some fraction of the flux of particles satisfying Eq. (12.2.3), i.e., lying above the nominal energy window or having the wrong polarity. It will shortly appear that this fraction is usually of the order of a few percent; hence this effect can be neglected unless the flux of particles within the nominal energy window is more than an order of magnitude smaller than the flux above or the flux of particles of opposite polarity, a situation which is not common but has occasionally been found to occur.[13,14]

12.2.2.1.2. ANGULAR RESPONSE. The most fundamental description of any detector is provided by the specification of its transmission function as a function of energy and direction of incidence. The transmission function (also known as the response function) is defined as the fraction of a beam of particles (of a given energy and direction, incident uniformly upon the entrance aperture) that is detected by the instrument; thus the measured current produced by a beam is equal to the flux density of the beam, times the area of the entrance aperture, times the charge of a single particle, times the transmission function.

In a modulated-potential Faraday cup the transmission function is determined primarily by (a) the modulating potential, which selects particles within a given range of velocities along the axis of the cup, as described earlier, and (b) the geometrical construction of the cup, which limits the range of angles from which particles can be accepted. The transparency of the grids and its variation with angle must also be taken into account. Figure 3 shows, as an example, the calculated transmission function of a Faraday cup flown on the IMP 2 satellite. As can be seen, the transmission function at a given angle is approximately constant over the energy range specified by Eq. (12.2.2) and at angles other than zero has a much smaller high energy "tail" as well as some response to particles of negative charge. At a given value of $E \cos^2 \theta$ the transmission function decreases uniformly with increasing angle and falls to zero, for typical cups, at an angle from the axis ranging from 45° to 60°.

The cylindrically symmetric construction of the usual Faraday cup implies that its transmission function depends only on energy and the polar angle with respect to the direction along the axis of the cup. As a result of this axial symmetry, the measurements provide no information on the azimuthal angle of incidence of the plasma. This limitation can be

[13] J. H. Binsack, *in* "Physics of the Magnetosphere" (R. L. Carovillano, J. F. McClay, and H. R. Radoski, eds.), p. 605. Reidel, Dordrecht, Holland, 1969.

[14] S. Olbert, *in* "Physics of the Magnetosphere" (R. L. Carovillano, J. F. McClay, and H. R. Radoski, eds.), p. 641. Reidel, Dordrecht, Holland, 1969.

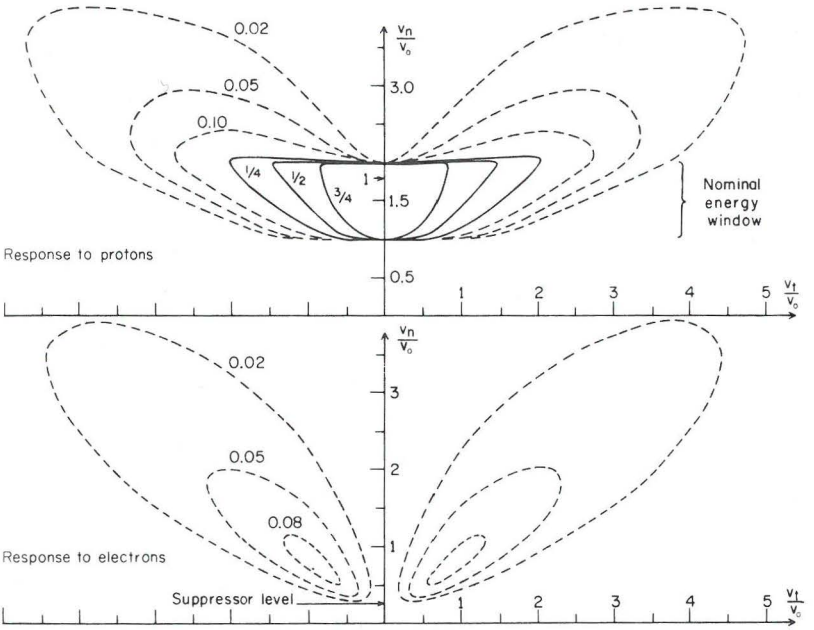

FIG. 3. Transmission function of a modulated-potential Faraday cup (similar to the one flown on IMP 2) operated in the positive ion mode. The transmission function, here and in subsequent figures, has been normalized so that its maximum value is unity. Shown are contours in velocity space of constant value of the normalized transmission function. The top figure is the response to positive particles, the bottom to negative particles, the detector in each case being operated in the positive ion mode. V_n is the velocity component along the normal to the entrance aperture, V_t the component transverse to it, and V_0 the speed corresponding to the bottom of the nominal energy window. The transmission function has rotational symmetry about the V_n axis. Dashed contours represent the 10% or less response due to the lateral displacements discussed in the text.

overcome to some extent by splitting the collector plate into several segments (usually two or three) and measuring the current from each segment separately. Figure 4 illustrates such a split-collector cup, used on the OGO satellites, and shows the dependence of its transmission function on direction. In some Faraday cups a "Venetian blind" collimator is placed in front of the entrance aperture in order to narrow down the angular opening of the transmission function to $\gtrsim 20°$ in the plane perpendicular to the collimator plates (but leaving the usual $\sim 50°$ width in the plane containing the plates).[15]

[15] A. J. Lazarus, H. S. Bridge, and J. Davis, *J. Geophys. Res.* **71**, 3787 (1966).

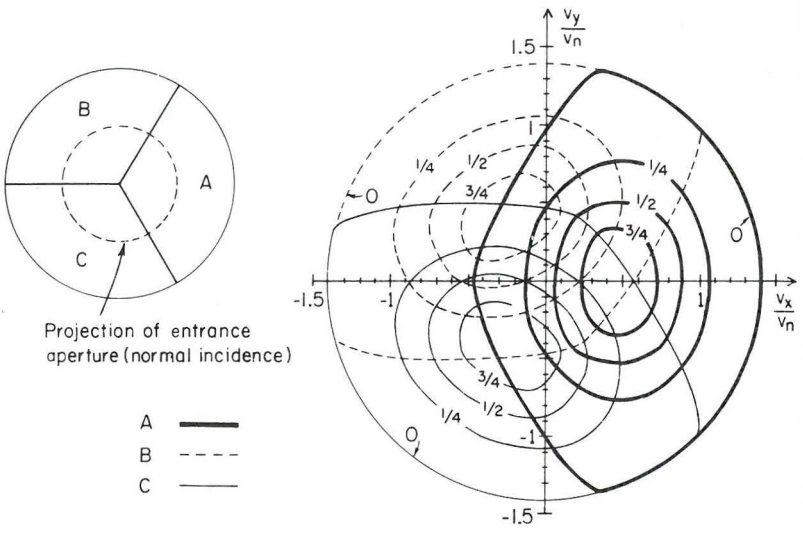

FIG. 4. (Left) A Faraday cup collector plate split into three segments (labeled A, B, C, respectively) to obtain some data on the azimuthal distribution of particle directions. (Right) Dependence of the normalized transmission function for the three collector segments on velocity transverse to the normal incidence direction. V_n is the velocity component along the normal to the entrance aperture and V_x, V_y are the transverse velocity components along axes x, y oriented relative to the collector segments as shown.

12.2.2.1.3. EXTRANEOUS EFFECTS. From extensive experience with modulated Faraday cups, both in laboratory testing and in spacecraft observation, it appears that when the cup is operated in the positive ion mode (i.e., with positive modulating potentials), its actual transmission function is adequately represented by the theoretical transmission function (such as that shown in Fig. 3) calculated from particle trajectories and cup geometry. In particular, the detector in this mode has no appreciable response to sunlight.[16] From the configuration of the potentials on the various grids, it is easily seen that only photoelectrons released from the suppressor grid can reach the collector; they, however, are not modulated and produce only an unmeasured steady current (historically this elimination of photocurrent effects from the suppressor grid was one of the principal reasons why the modulated-potential Faraday cup was developed[10]).

On the other hand, when the detector is operated in the electron mode (with negative modulating potentials), several additional sources of

[16] A. Bonetti, H. S. Bridge, A. J. Lazarus, B. Rossi, and F. Scherb, *J. Geophys. Res.* **68**, 4017 (1963).

alternating currents not included in the theoretical transmission function may be present. In this mode the detector is strongly sensitive to sunlight, which produces alternating currents as large as or larger than typical electron currents to be measured; successful observation of electrons has so far only been possible with the detector facing well away from the sun.[17] The source of these modulated photoelectron signals is not well understood, but they are thought to be produced by photoelectrons released from the modulator grid. Two mechanisms by which these photoelectrons can be modulated have been proposed: (a) the fraction of photoelectrons moving toward the collector (rather than out the entrance aperture) may be affected by the strong inhomogeneous electric fields immediately adjacent to the grid wires, which vary with the modulator potential; (b) the photoelectrons strike the suppressor grid with an energy per charge essentially equal to the difference between the suppressor and modulator potentials (thus varying periodically with the modulator potential) and produce a secondary electron flux that is modulated because the secondary electron yield (number of secondaries per primary) varies with the primary electron energy.

Furthermore, in the electron mode the detector has a sensitivity to protons that arises because the protons strike the modulator grid at an energy/charge that is the sum of the modulator potential and the proton energy/charge outside the detector; as in (b) above, this gives rise to a modulated secondary electron current.[17,18] Since the secondary electron yield for protons striking a metal surface is approximately linear with proton energy (up to energies of $\sim$10 keV),[19] the modulated secondary electron flux is proportional to the difference between the upper and lower limits of the modulator potential and is independent of the proton energy; it is also in phase with the modulation rather than 180° out of phase, allowing the occurrence of the effect to be recognized. The magnitude of this modulated current is approximately one percent of the incident proton current for a modulation potential range of 1 kV,[17] and in practice it is important only within regions having a very high proton density, such as the plasmasphere (refer to Fig. 1). The effect could be suppressed by placing in front of the modulator another grid with a steady positive potential large enough to repel the incoming protons.

Finally, incoming electrons detected by the cup produce secondary electrons at both the modulator and suppressor grids; the secondary flux is proportional to the primary flux and hence is modulated along with

[17] V. M. Vasyliunas, *J. Geophys. Res.* **73,** 2839 (1968).
[18] J. H. Binsack, *J. Geophys. Res.* **72,** 5231 (1967).
[19] D. B. Medved and Y. E. Strausser, *Advan. Electron. Electron Phys.* **21,** 101 (1965).

it. The main effect is simply to enhance the incident electron current by an amount ranging up to 10%, depending on the electron energy.

12.2.2.2. The Curved-Plate Analyzer—General Description. The curved-plate electrostatic analyzer was developed as a laboratory instrument long before the era of space exploration (see references in the work of Paolini and Theodoridis[20]). Its general form is shown schematically in Fig. 5. It consists of two parallel curved plates, which are segments either

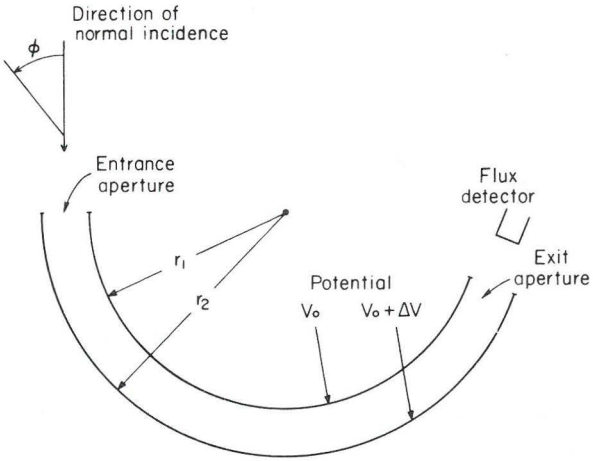

FIG. 5. Schematic diagram of a curved-plate analyzer.

of a cylinder or of a sphere, with a potential difference between them (in typical space applications, the radii of curvature of the plates are of the order of 10 cm and the separation between the plates is of the order of 1 cm or less). A charged particle entering the entrance aperture at normal incidence will move in a circular orbit of radius r if its kinetic energy E (when inside the analyzer), charge q, the potential difference between the plates ΔV, and the radii of curvature of the inner and outer plates, r_1 and r_2, are related by the equation

$$2E = q\,\Delta V/\log(r_2/r_1) \tag{12.2.5}$$

for a cylindrical analyzer, or

$$2E = q\,\Delta V/r\left(\frac{1}{r_1} - \frac{1}{r_2}\right) \tag{12.2.5a}$$

[20] F. R. Paolini and G. C. Theodoridis, *Rev. Sci. Instrum.* **38,** 579 (1967).

for a spherical analyzer (evidently $r_1 < r < r_2$). If $r_1 \equiv r_0 - \frac{1}{2}\Delta r$, and $r_2 \equiv r_0 + \frac{1}{2}\Delta r$, then to lowest order in $\Delta r/r_0 \ll 1$ both equations reduce to

$$2E \simeq q\,\Delta V r_0/\Delta r. \qquad (12.2.5b)$$

Particles which are incident at a direction sufficiently different from normal or whose energies differ sufficiently from the value given by Eq. (12.2.5) will strike one or the other of the plates before reaching the exit aperture. Thus the flux of particles out of the exit aperture corresponds to the flux of incident particles within a narrow range of energies and directions (in the plane perpendicular to the plates). This steady flux of particles can be detected either by measuring the current to a collector plate or by counting pulses from a single particle detector.

It should be noted that the kinetic energy E in Eqs. (12.2.5) is the energy the particle has while inside the analyzer. Unless the particle crosses the entrance aperture at the unique point (if it exists) whose potential with respect to points far outside is zero, E is not equal to the particle's energy outside the analyzer. The change in energy is brought about by acceleration in the fringing fields at the entrance aperture, which thus necessarily play a role in determining the transmission function of the analyzer; in particular, from Eq. (12.2.5b) it at once follows that, if the width of the entrance aperture is equal to the separation of the plates (as it usually is in space applications), the range of (outside) particle energies accepted by the analyzer is at least equal to $q\,\Delta V$.

12.2.2.2.1. SURVEY OF VARIOUS GEOMETRIES. The principal properties characterizing a particular curved-plate analyzer are:

(1) Type of plates (spherical or cylindrical).

(2) Ratio of plate spacing to mean radius of curvature ($\Delta r/r_0$ in Eq. (12.2.5b); values ranging from 0.03 to 0.1 have been used in space work.

(3) Length of the plates, usually expressed as an angle (180° corresponds to half a sphere or cylinder, etc.).

(4) Potential of the plates with respect to distant points. A "balanced" analyzer has a potential $-\frac{1}{2}\Delta V$ on the inner plate and $+\frac{1}{2}\Delta V$ on the outer plate, to look at positive ions (the reverse to look at electrons), so that zero potential is midway between the plates. Any other arrangement gives an "unbalanced" analyzer. The main advantage of balanced analyzers is that they minimize the fringing field effects mentioned earlier; on the other hand, they can measure particles of a given polarity only (plate potentials must be interchanged to measure particles of the other polarity). The one type of unbalanced analyzer in spacecraft use [see (d) following] has three plates, the middle one at a potential $+\Delta V$ and the outer two

grounded; the inner pair of plates thus forms an analyzer for protons and the outer pair for electrons.

By varying these properties a large number of different analyzer designs can be obtained. Four main types have been used on spacecraft to date:

(a) Cylindrical plates, 120° in length, balanced. Example: Mariner 2 (see Table II).

(b) Hemispherical: 180°-long spherical plates, balanced (e.g., Vela satellites).

(c) Quadrispherical: 90°-long spherical plates, balanced (e.g., Pioneer 6, 7, 8).

(d) Cylindrical 43° plates, unbalanced three plate arrangement described above (e.g., OGO 3, 5); this is the "Low Energy Proton and Electron Differential Energy Analyzer" or LEPEDEA, developed at the University of Iowa.[21,22] In later versions of this instrument,[23] the plate potential is not steady but is modulated at a frequency of 2.4 kHz by a triangular waveform having an amplitude of 25% of the mean value; since the modulation period is long compared to the transit time of the particles through the analyzer yet short compared to the integration time of the particle detector at the exit aperture, the result is simply to broaden the energy response of the instrument by 25% over that obtained with a fixed plate potential.

Most curved plate analyzers accept particles within a narrow range of angles in the plane perpendicular to the plates (azimuthal angles) but over a wide range in the plane tangent to the plates at the entrance aperture (polar angles). Quadrispherical analyzers [type (c) above] developed at the NASA Ames Research Center were designed to measure simultaneously the particle flux as a function of polar angle, by means of the scheme illustrated in Fig. 6.[24] A relatively narrow entrance aperture is used, but a wide collector plate is placed at the exit aperture and split into a number of separate segments; the current from each segment corresponds to the flux of particles entering the analyzer within a particular narrow range of polar angles. The quadrispherical geometry is essential for this measurement; in a hemispherical analyzer, for instance, particles entering at a particular point on the aperture but at different polar angles will all converge again to a single point after traversing the half sphere.

[21] L. A. Frank, Univ. of Iowa Rep. 65–22. Univ. of Iowa, Iowa City, Iowa, 1965.

[22] L. A. Frank, *J. Geophys. Res.* **72,** 185 (1967).

[23] L. A. Frank, W. W. Stanley, R. H. Gabel, D. C. Enemark, R. F. Randall, and N. K. Henderson, Univ. of Iowa Rep. 66–31. Univ. of Iowa, Iowa City, Iowa, 1966.

[24] J. H. Wolfe, R. W. Silva, D. D. McKibbin, and R. H. Mason, *J. Geophys. Res.* **71,** 3329 (1966).

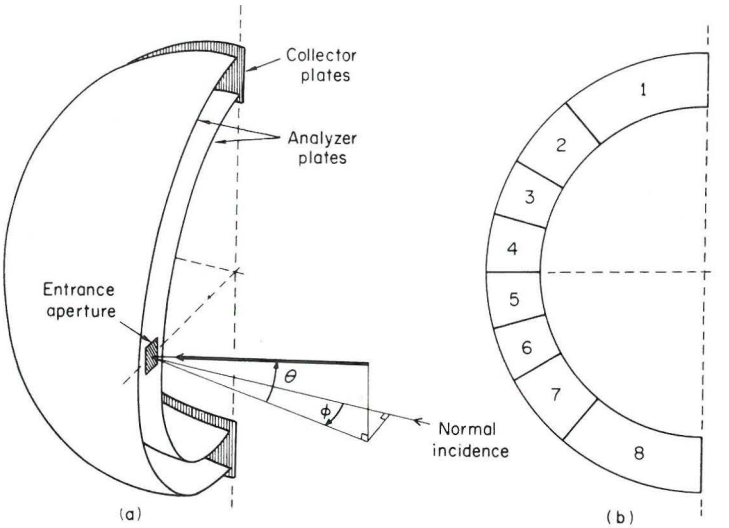

FIG. 6. Schematic diagram of (a) a quadrispherical curved-plate analyzer with (b) a multi-segment collector (face-on view) designed to measure the particle distribution as a function of polar angle θ.

12.2.2.2.2. THE COUPLED ENERGY-ANGULAR RESPONSE. Figure 7 illustrates the transmission functions of several curved-plate analyzers used for solar wind observations. An intrinsic feature of all curved-plate analyzers, readily apparent in Fig. 7, is the energy-angle asymmetry or "skewing": the range of energy of particles accepted by the analyzer is a strong function of azimuthal angle ϕ, moving upward with increasing angle (in the sense indicated in Fig. 5); the transmission function appears markedly "tilted" from the normal incidence direction in velocity space. The effect arises because particles entering the analyzer with their velocity vectors directed toward the inner plate must have a higher energy to be transmitted than particles with their velocity vectors directed toward the outer plate. The magnitude of the "skewing" increases with increasing ratio of plate spacing to radius and is more pronounced for a quadrispherical than for a hemispherical analyzer. The existence of this strong coupling between energy and angle required for acceptance implies that a curved-plate analyzer cannot in general be characterized merely by an "energy bandpass" and "angle of acceptance."

If the only potentials in the analyzer are $\pm\frac{1}{2}\Delta V$ on the two plates or ΔV on one plate and ground on the other, it is readily shown by scaling the equations of motion that the transmission function depends only on angles and on the ratio $E/q\ \Delta V$, i.e., the energy dependence scales with the plate potential. This implies that, if at a particular angle particles with

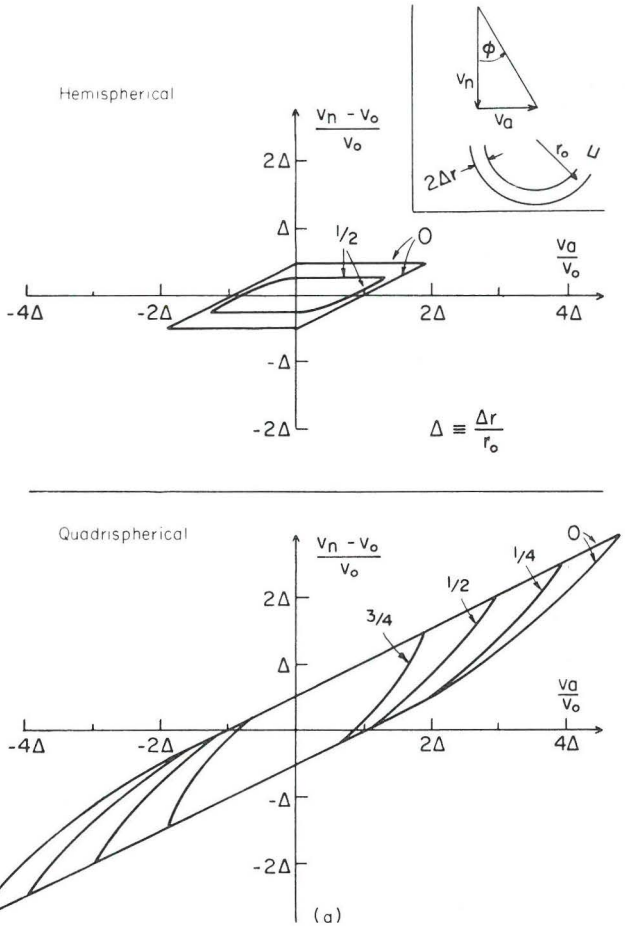

FIG. 7a. Normalized transmission functions of a hemispherical (top) and quadrispherical (bottom) curved-plate analyzer; dependence on normal and azimuthal velocity components (defined as shown in insert). V_0 is the speed corresponding to the energy defined by Eq. (12.2.5b). (From theoretical calculations, kindly provided by A. J. Hundhausen.)

energies between, say $E - \frac{1}{2}\Delta E$ and $E + \frac{1}{2}\Delta E$ are accepted, then $\Delta E/E$ is a constant, independent of the plate potential and depending only on the geometry of the analyzer (it can be shown that $\Delta E/E$ is proportional to $\Delta r/r_0$ if it is small). This result is unaffected by the presence of fringing fields; any departures from it imply that either some potential other than the ΔV on the plates is present (for example, postaccelerating

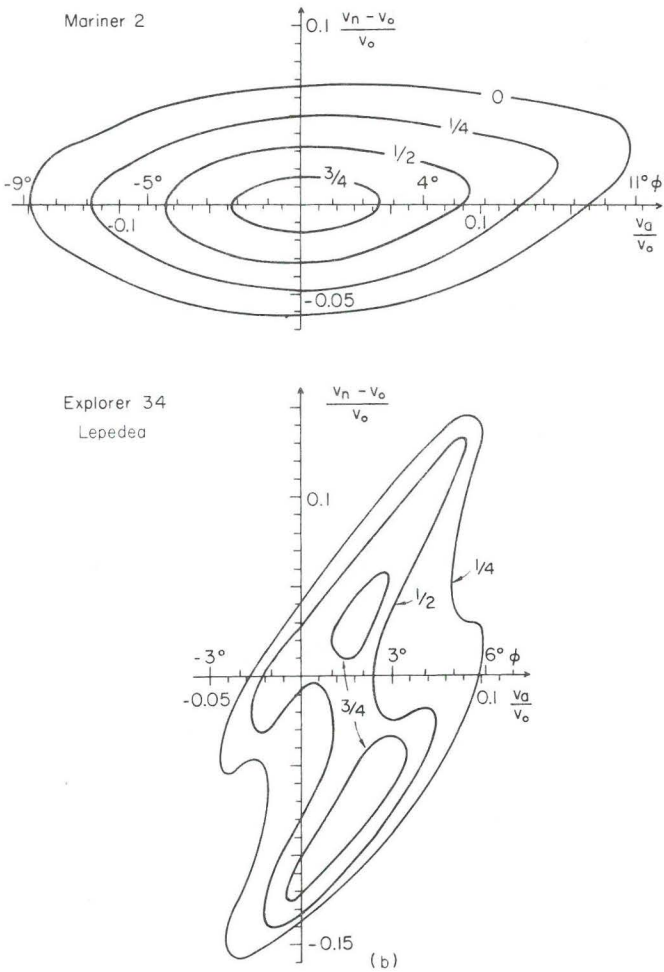

FIG. 7b. Normalized transmission functions of cylindrical curved-plate analyzers; dependence on normal and azimuthal velocity components. (Top) Response of Mariner 2 analyzer [constructed from data by M. Neugebauer and C. W. Snyder, *J. Geophys. Res.* **71,** 4469 (1966)]. (Bottom) Response of channel 6B of LEPEDEA analyzer with modulated plate voltage flown on Explorer 34 (constructed from laboratory calibration curves given by L. A. Frank, W. W. Stanley, R. H. Gabel, D. C. Enemark, R. F. Randall, and N. K. Henderson, Univ. of Iowa Rep. 66–31. Univ. of Iowa, Iowa City, Iowa, 1966.) V_0 corresponds to an energy of 1 keV.

potentials after the exit aperture) or that effects not included in the equations of classical mechanics (e.g., secondary emission or scattering of particles from plates) are occurring.

12.2.2.2.3. EXTRANEOUS EFFECTS. Many of the instruments used to detect particles coming out of the exit aperture are sensitive to sunlight. Because of the curvature of the plates, light cannot reach the detector directly, but in practice it might reach the detector by scattering from the plates; to prevent this, the inside surfaces of the analyzer are usually blackened. It is also possible to construct that portion of the plates struck by direct sunlight out of a highly transparent grid (instead of a solid metal) and to place a light trap behind it.[11]

Two other effects that may be important, especially in analyzers used to observe electrons, are the scattering of electrons from the plates and the production of secondary electrons near the end of the plates. In some instruments the plates are machined with narrow (approximately 0.1 cm) serrations to suppress scattering (and also reflection of light). Secondary electron emission may be reduced or suppressed by placing a negative grid after the exit aperture, or some other negative electrode (e.g., a negative ring in the Mariner 2 analyzer) that can prevent low-energy electrons released at the plates from reaching the particle detector. Alternatively, electron scattering and secondary production may be allowed but their effect estimated from laboratory calibration and included in the specification of the transmission function.

12.2.2.3. The Crossed-Field Velocity Selector. An instrument capable of measuring separately the energy spectra of protons and alpha particles has been developed by the Goddard–University of Maryland group.[11,12] A cylindrical curved-plate analyzer (similar to those described in the previous section) selects ions within a narrow range of energy per charge; particles leaving the exit aperture of the analyzer then enter a crossed electric and magnetic field velocity selector (Wien filter) tuned to a velocity corresponding to the energy per charge of the ion species being observed. With the instrument set to observe alpha particles, the proton contamination is less than 0.3%, and vice versa. A detailed description of the velocity selector, including a discussion of the design requirements imposed by spacecraft use (chiefly the necessity for a permanent magnet and a severe restriction on the total length of the device) has been published.[12]

12.2.2.4. Comparison of Instruments

12.2.2.4.1. ENERGY RANGE. An upper limit to the energy of particles that can be detected is set by the highest available voltage. Voltages up to ~ 10 kV have been successfully attained in detectors flown to date. Hence a modulated-potential Faraday cup, which requires a voltage as large as the energy per charge of the particles being observed, is at present limited to protons and electrons having energies under 10 keV; this is generally adequate for observations within the solar wind but not within some

regions of the outer magnetosphere. On the other hand, a curved-plate analyzer requires a plate voltage which, in typical space instruments, is of the order of 10% of the particle energy per charge; thus it can observe particles up to 50–100 keV, overlapping the energy range accessible to high-energy instruments such as the thin-window Geiger tube (which can detect electrons above ~40 keV) (see, e.g., Frank and Van Allen[25]) or the scintillation counter (electrons above ~20 keV, protons above ~100 keV) (see, e.g., Davis and Williamson[26]).

12.2.2.4.2. DIFFERENTIAL VERSUS INTEGRAL MEASUREMENTS. The curved-plate analyzer is an intrinsically differential instrument, measuring particles within a narrow range of energies and angles. A very narrow response enables one to study in some detail the velocity space structure of very narrow particle distributions such as are found in the solar wind. Since the location of such sharp peaks in velocity space is not, however, *a priori* known and may be variable, the narrow energy-angle ranges sampled by the various detector channels must be contiguous and hence the required number of channels is quite large; if there are appreciable gaps in either energy or angle coverage, a significant fraction of the particle distribution may not be observed by the detector, with consequent large errors in estimates of total particle flux. On the other hand, modulated Faraday cups used to date have had relatively wide energy and angular windows (it should be understood, however, that this is not necessarily an intrinsic characteristic of this detector; energy windows as narrow as 2% are to be used in some future instruments,[27] and in principle the angular response could be narrowed down to a few degrees with collimators). The wide response makes it possible to cover a large part of velocity space with a relatively small number of contiguous windows and to obtain reliable total flux measurements no matter how narrow the particle distribution. The question of differential versus integral functioning of detectors is further discussed in Section 12.3.2.

It should also be noted that the ratio $\Delta E/E$ discussed earlier is generally fixed by the geometry in a curved-plate analyzer, whereas it can be electronically varied in a modulated-potential Faraday cup by varying the width of the modulator voltage relative to the mean level.

12.2.2.4.3. SENSITIVITY. The entrance aperture of a Faraday cup can be made quite large, since its maximum diameter is limited only by the size of the entire instrument. The curved-plate analyzer, on the other hand, requires a plate separation small compared to their radius and hence has a

[25] L. A. Frank and J. A. Van Allen, *J. Geophys. Res.* **68,** 1203 (1963).

[26] L. R. Davis and J. M. Williamson, *Space Res.* **3,** 365 (1963).

[27] J. Binsack, Private communication, 1968.

rather small entrance aperture. The effective collecting area of a typical Faraday cup is thus at least two orders of magnitude larger than that of a typical curved-plate analyzer; this is somewhat offset by the greater sensitivity of flux measurement methods used with curved-plate analyzers (see Section 12.3). Taking into account both the collecting area and the flux detection sensitivity, the minimum detectable particle flux density is of the same order of magnitude both for a Faraday cup and for a curved-plate analyzer that uses current collector plates for particle detection. The introduction of particle-counting methods in curved-plate analyzers allowed a considerable lowering of the minimum detectable flux level for a given collecting area or, alternatively, a reduction of collecting area for a given flux level. Initially the second alternative was taken: plate separation (and hence the collecting area) was reduced in order to obtain an increase in resolution,[1] without a major gain in sensitivity. In analyzers of the LEPEDEA class, however, particle counting was combined with a relatively wide plate spacing to obtain a minimum detectable flux level two orders of magnitude below that of previous instruments[22] (although at the expense of a greatly enhanced "skewing" of the transmission function).

12.2.2.4.4. Absolute Calibration. The relatively simple construction of the Faraday cup allows a reliable theoretical calculation of its transmission function, which can be verified by simple laboratory tests; hence the absolute efficiency for the detection of positive ions is known with great certainty. On the other hand, the complicated response of the curved-plate analyzer and the unavoidable presence of significant fringing fields make it difficult to obtain theoretically a useful transmission function, which must then be determined by laboratory calibration (discussed further in Section 12.2.4). The calibration must be detailed enough to determine the complete shape of the transmission function, including the energy-angle "skewing" discussed earlier; knowledge of merely an "energy width" and "angular width" is not adequate. In the absence of such a calibration, the absolute efficiency of the analyzer may be rather uncertain.

On the other side of the ledger, a Faraday cup operated in the positive ion mode has a slight sensitivity to electrons (already discussed in Section 12.2.2.1.1), which under some conditions is significant and must be taken into account[13,14] (in the solar wind and the magnetosheath, however, it can be eliminated almost entirely by setting the negative suppressor grid potential at a value $\gtrsim 100$ volts, large enough to prevent most of the plasma electrons from reaching the collector); such "contamination" is not present in a curved-plate analyzer.

12.2.3. Flux Measurement

In this section we briefly describe the principal methods used to measure the flux of particles striking the collector plate or leaving the exit aperture of the instruments described. Only the basic features will be treated, not the detailed electronic circuitry (detailed descriptions of the electronics for several of the instruments are available as technical reports[28–30]).

12.2.3.1. Direct Current Methods. Curved-plate analyzers that use collector plates as detecting elements measure the direct current from the plates by means of electrometers. Typical instruments have a minimum detectable current of 10^{-14}–10^{-13} A, a minimum integration time of the order of 0.1 sec, and a dynamic range varying from 4 to 7 decades. The measurement is transmitted to a tracking station either in digital form (generally as a binary number of 6–8 bits) or in analog form (generally with at most a few percent precision) depending on the spacecraft telemetry system. Since neither method allows the transmission of a number with a 4-decade range and since the construction of a signal processing system linear over several decades is very difficult, the value of the collector current is not itself the telemetered quantity; instead, the electrometer is designed so that its output is proportional to the logarithm of the input current.

12.2.3.2. Alternating Current Methods. The measured output of a modulated-potential Faraday cup is an alternating current of known frequency and phase. The measurement is accomplished by coupling the collector plate to the signal processing system through a capacitor, then passing the ac signal through a preamplifier, through a narrow-band filter tuned to the known frequency, and through a compression amplifier that produces an output approximately proportional to the logarithm of the input current (for the same reasons as in the case of the dc electrometers discussed above). The ac signal finally must be rectified; in the early instruments this was accomplished with a simple full-wave rectifier circuit, but at present a synchronous detector is generally used to exploit the fact that the phase of the signal is known (this results in a very narrow bandwidth and a consequent reduction of the noise level). Typical integration times, in the instruments flown to date, are of the order of tens of milliseconds (considerably shorter than those of the dc electrometers).

[28] E. F. Lyon, Lincoln Lab. Rep. 52G–0017. Lincoln Lab., M.I.T., Cambridge, Massachusetts, 1961.

[29] C. Josias and J. L. Lawrence, Jr., Tech. Rep. 32–492. Jet Propulsion Lab., Pasadena, California. 1964.

[30] Final Engineering Report for the M.I.T. Plasma Experiment on Pioneer 6 and Pioneer 7. M.I.T. Lab. for Nucl. Sci., Cambridge, Massachusetts, 1967.

The minimum detectable current at present is near or somewhat below 10^{-12} A; this limit is largely due to thermal noise in the circuits.

12.2.3.3. Counting Methods. More recent curved-plate analyzers do not measure currents but instead count individual particles leaving the exit aperture. The low energy (down to 100 eV and below) of the particles requires that they be detected without traversing any appreciable amount of matter; thus traditional counting methods such as Geiger tubes and scintillation counters are not usable (the thin-window Geiger tube extensively used in radiation belt observations, for instance, requires particles to penetrate 1.2 mg/cm^2 of matter, which limits it to electron energies above 40 keV). Particle detection is usually accomplished with some form of electron multiplier. In the multipliers used on the Vela satellites,[31] the particle hits a sensitive surface, producing secondary electrons which then cascade from electrode to electrode in the same manner as in the conventional photomultiplier. A more recent and simpler instrument of the multiplier type is the continuous channel multiplier (Bendix "channeltron").[32] The counting efficiency of all these instruments (ranging from approximately 10% to nearly 100% for particle energies usually encountered) must generally be determined by laboratory calibration; there also may be possible changes in efficiency with time and/or total charge collected, which may be particularly significant in the case of the channeltron.[33]

Another particle-counting system, developed by the Goddard–University of Maryland group,[11] postaccelerates the positive ions and lets them strike an aluminum target, producing secondary electrons (the postacceleration is achieved by placing a large negative potential on the suitably shaped target); the secondary electrons are then repelled by the negative potential of the target and strike a scintillator with enough energy to be counted. This system is intrinsically limited to the detection of positive particles and cannot be adapted to detect electrons.

The sole instance to date of counting methods used in conjunction with a Faraday cup is an instrument developed at Rice University.[34] A funnel-shaped continuous channel electron multiplier is the particle counter. The quantity measured is the number of counts when the modulator potential is high minus the number of counts when it is low; the value of this quantity is on the average proportional to the flux of particles with

[31] S. Singer, *Proc. IEEE* **53,** 1935 (1965).

[32] D. S. Evans, *Rev. Sci. Instrum.* **36,** 375 (1965).

[33] S. Cantarano, A. Egidi, R. Marconero, G. Pizzella, and F. Sperli, *Ric. Sci.* **37,** 387 (1967).

[34] J. W. Freeman, Jr., *J. Geophys. Res.* **73,** 4151 (1968).

energies per charge within the range defined by the upper and lower limits of the modulator potential, as in the conventional modulated Faraday cup. This method has the disadvantage that when most of the particles lie above the nominal energy window of the detector, the measured quantity is the small difference between two large counting rates and hence is subject to large statistical fluctuations. Such large fluctuations have actually been observed, and in fact used to detect the presence of large fluxes of particles above the energy range of the instrument.[35] (This problem does not arise with conventional modulated Faraday cups since the precision of the ac measurement is unaffected by the presence of direct currents due to unmodulated higher energy particles.)

12.2.4. Calibration

Before being placed on the spacecraft, plasma detectors are usually calibrated in the laboratory in order to determine the transmission function (or else to check a theoretically calculated one). Since all these instruments are simply detectors of particle beams rather than plasma detectors in the conventional sense, they can be calibrated by exposing them to particle beams obtained with standard beam technology; there is no need for the difficult task of producing an actual plasma, let alone one which would simulate solar wind conditions. Some special precautions should, however, be observed. The particle fluxes encountered by the detector are expected to be uniform over its entrance aperture; hence the calibration must be performed with effectively uniform illumination of the entrance aperture, obtained either directly with a wide, uniform beam or by scanning a narrow beam across the entire aperture. The spread of the beam in energy and angle must be small compared with the width of the transmission function; particularly with the complex and very narrow transmission functions of curved-plate analyzers, this requires beams with an energy spread $< 1\%$ and an angular divergence $\lesssim 1°$.

12.2.5. Organization of Energy and Angle Measurements

The instruments described in the preceding sections can at any one time detect particles only within a limited range, centered about some mean value, of energy and angle. The mean energy can be varied by varying a suitable voltage in the instrument; usually the voltage is varied in preprogrammed steps (each step is often referred to as an "energy window" or "energy channel"). The angle can in principle be varied by

[35] J. W. Freeman, Jr., C. S. Warren, and J. J. Maguire, *J. Geophys. Res.* **73,** 5719 (1968).

varying the orientation of the detector and, to a more limited extent, by making use of various split-collector arrangements or by using several separate instruments looking in different directions. In designing a detector to be flown on a particular spacecraft, a set of energies and angles at which measurements are to be made must be selected and sequenced; this set must both be able to provide the desired information and be compatible with the limited capacity of the spacecraft telemetry. This section describes the principal schemes of organizing the complete set of energy and angle measurements. (For references to specific spacecraft, see Table II.)

12.2.5.1. Instruments on Spin-Stabilized Spacecraft. Many spacecraft are designed to spin stably about an axis fixed in inertial space. The typical spin period is of the order of a few seconds; for spacecraft intended to study the solar wind, the spin axis is usually oriented at a large angle to the ecliptic plane (the plane of the earth's orbit about the sun). A spinning spacecraft provides an easy method of varying the orientation of the detector, which is therefore mounted so that the normal to its entrance aperture forms a large angle (usually 90°) with the spin axis. The simplest scheme of taking measurements, and the one first used successfully, consists of maintaining a fixed energy window during one complete revolution of the spacecraft and measuring the flux as a function of angle (typically at 20 or so equally spaced angles); then the instrument is advanced to the next energy window and again during one revolution a complete angular scan is made, and so on until the instrument has cycled through all of its energy windows. This provides a complete two-dimensional set of measurements of flux as a function of energy and angle of azimuth about the spin axis (the dependence on polar angle can only be observed by such means as split collectors).

In the solar wind appreciable fluxes of protons are observed coming only from directions within a small range ($\sim 20°$) of the radius vector from the sun, and hence taking measurements at equally spaced angles is rather inefficient. Instruments designed primarily for study of the solar wind thus take many measurements at angles looking close to the sun and only a few (or else integrated over wide angular intervals) looking away from the sun. This scheme, of course, is possible only if the spacecraft is equipped with a sun sensor capable of indicating to the instrument when it is looking at the sun.

Another scheme, used with Faraday cups on Explorer 33 and 35 satellites, measures the total flux of protons (using a very wide energy window) as a function of angle, during one revolution, and also picks out the angle at which the maximum flux is coming; during succeeding

revolutions it then measures the flux at that one angle as a function of energy. This provides two one-dimensional sets of measurements: total flux (integrated over energy) as a function of angle, and flux at one angle as a function of energy.

In all the schemes described so far, the time required to obtain a complete set of measurements (often called a complete "spectrum") is equal to the spin period times the number of energy channels, typically ~ 1 min. The interval between consecutive spectra could in principle be as short as the time required for one spectrum, but in practice it often is longer because of telemetry limitations.

A somewhat different scheme has to be used on spacecraft which rotate very slowly (such as Vela 4, which has a spin period of about 1 min). In this case the sequence of energy and angle measurements is reversed: the fluxes in all the energy windows are measured successively, as rapidly as possible and hence all at essentially one angle; this is then repeated at other angles, and a complete energy-angle scan is obtained during one (in this case rather long) revolution of the spacecraft.

A convenient way of labeling a single measurement at a particular energy and angle is to specify the mean energy per charge E/q accepted by the particular energy window and the angles (θ, ϕ) which define the normal direction of the entrance aperture with respect to some fixed (i.e., not rotating with the spacecraft) coordinate system; one may then define a corresponding speed u by the equation

$$e|E/q| = \tfrac{1}{2}mu^2,$$

where e is the elementary charge and m the mass of the proton (or the electron if negative particles are being measured), and consider the triplet of numbers (u, θ, ϕ) as a vector $\mathbf{u}$ of magnitude u and direction given by (θ, ϕ). (In principle a third angle ψ, the angle of rotation of the detector about its normal direction, should also be specified if the detector's transmission function is not axially symmetric, but in nearly all cases occurring in practice the motion of the detector is constrained so that ψ is a unique function of θ and ϕ.) Then each measurement corresponds to a single "velocity" vector $\mathbf{u}$ and can be thought of as a point in $\mathbf{u}$ space. The various sampling schemes discussed above can then be succinctly represented by series of points in the plane in $\mathbf{u}$ space perpendicular to the spacecraft spin axis. These representations are illustrated in Fig. 8.

12.2.5.2. Instruments on Triaxially Stabilized Spacecraft. Some spacecraft (notably the Mariner series and the later satellites in the OGO series) do not spin but maintain a fixed orientation in space, with only very slow,

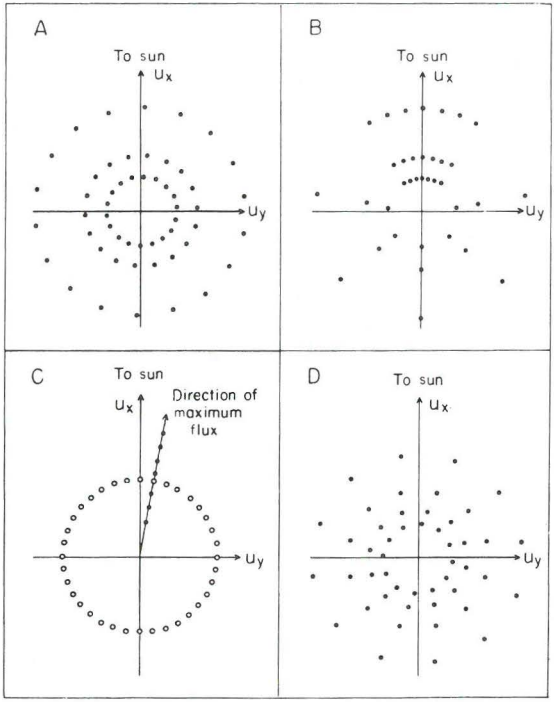

FIG. 8. Sampling schemes for energy and angle measurements on rotating spacecraft. (A) Measurements made at equally spaced angles for each energy window. (B) Measurements concentrated at angles close to the solar direction. (C) The Explorer 33–35 scheme: open circles represent measurements in very wide ("integral") energy windows; dots represent measurements in narrow ("differential") energy windows. (D) Measurements on a slowly rotating spacecraft.

long-term changes. Hence if measurements of flux as a function of angle are desired, they must be made by means of split-collector or multiple-detector arrangements (scanning by means of mechanical motion of the detector is, in principle, also possible but to date has not been successfully realized), and the amount of angular information available from these spacecraft is generally quite inferior to that from spin-stabilized spacecraft. On the other hand, a much higher time resolution in the measurement of flux as a function of energy at a fixed angle is possible since one is not constrained to wait a full rotation before advancing the instrument from one energy step to the next. (Alternatively, a much longer integration time for a single measurement is possible.)

12.3. Methods of Analysis

12.3.1. Nature of Information To Be Obtained

In this section we discuss how and what information about the plasma can be obtained from measurements of currents or counting rates at various energies and angles. Referring back to Table I, we note that all extraterrestrial plasmas accessible to direct measurement are collisionless, in the sense that the mean free path for Coulomb collisions is much longer than the characteristic macroscopic length scales. Hence there is no *a priori* reason to expect any kind of thermodynamic equilibrium or applicability of the temperature concept; a complete description of the plasma requires the specification of the velocity distribution function for each species of particles present. Nevertheless, it has been found empirically that, at least in the solar wind and the magnetosheath, the plasma can be described to a surprisingly adequate extent for many purposes by specifying only its hydrodynamic parameters: density, bulk velocity, pressure tensor, and (sometimes) heat flux vector.[1,14] (These may have to be specified separately for each species of particles; physical considerations require that the number densities and bulk velocities of positive and negative particles to a very high approximation be equal, but the pressures and heat fluxes for individual species may very well be different and have in fact been observed to be different.[1,7]) Much of the analysis of extraterrestrial plasma measurements consists of determining these hydrodynamic parameters of the plasma, which of course are simply the moments of the velocity distribution function $f(\mathbf{v})$: if n is the number density, $\mathbf{V}$ the bulk velocity, $\mathbf{P}$ the pressure, and $\mathbf{q}$ the heat flux, then these are *defined* for each species by

$$\begin{aligned} n &= \int d\mathbf{v}\, f(\mathbf{v}), \\ n\mathbf{V} &= \int d\mathbf{v}\, \mathbf{v} f(\mathbf{v}), \\ \mathbf{P} &= m \int d\mathbf{v}\, f(\mathbf{v})(\mathbf{v} - \mathbf{V})(\mathbf{v} - \mathbf{V}) \\ \mathbf{q} &= \tfrac{1}{2} m \int d\mathbf{v}\, f(\mathbf{v})(\mathbf{v} - \mathbf{V}) \mid \mathbf{v} - \mathbf{V} \mid^2 \end{aligned} \tag{12.3.1}$$

(where the integrals are volume integrals over velocity space). All extraterrestrial plasmas contain a magnetic field and the pressure tensor is usually assumed to be axially symmetric:

$$\mathbf{P} = P_\perp \mathbf{I} + (P_\parallel - P_\perp)\mathbf{bb}$$

where **I** is the unit dyadic and **b** is the unit vector in the direction of the field. The "temperature" is simply defined, for convenience, as the ratio $kT \equiv \mathbf{P}/mn$ and is thus also a tensor; the use of the term "temperature" does not in any way imply the existence of thermal equilibrium or a Maxwellian velocity distribution. (The reader, however, should beware of some observational papers in which the word "temperature" is applied to various specialized measures of velocity dispersion having only a vague connection with the term as used in plasma physics.)

Besides the moments of the distribution function, its detailed structure is also of interest but can generally be studied only in regions of space, such as the magnetosheath and especially the outer magnetosphere, where the distribution function is very broad in comparison with the transmission functions of available detectors.

12.3.2. Relation of Measurements to the Particle Distribution Function

The raw data obtained from a plasma detector on a spacecraft consists of a sequence of currents or counting rates at various energy windows and angular orientations of the detector. It is convenient to specify the energy and angle of each measurement by the vector **u** described in Section 12.2.5.1. If $C(\mathbf{u})$ is the counting rate of the detector during a particular measurement, then the contribution to it of particles of a given velocity is equal to the number of particles at that velocity, times the component of velocity normal to the entrance aperture, times the area of the entrance aperture, times the transmission function. (We are now assuming that, as discussed in Section 12.1.2, the flux on the entrance aperture represents the plasma particle flux unaffected by the spacecraft and hence is uniform over the aperture, which is much smaller than any length scale of the plasma.) To obtain the total counting rate it is necessary to sum the contributions from all velocities and all species of particles (unless the instrument is designed to accept only one species), which means an integral over velocity space weighted by the sum of velocity distribution functions for all species. Thus (assuming that the counting efficiency for particles of each species is the same), we obtain the equation

$$C(\mathbf{u}) = S \sum_a \int d\mathbf{v}\, v_n G(\mathbf{u}(Z_a/A_a)^{1/2}, \mathbf{v}) f_a(\mathbf{v}) \qquad (12.3.2)$$

where Z_a and A_a are the atomic mass numbers of the ath species, S is the area of the entrance aperture, $v_n \equiv \mathbf{v} \cdot \mathbf{u}/u$ is the velocity component normal to the entrance aperture, $f_a(\mathbf{v})$ is the velocity distribution function of particles of the ath species, and $G(\mathbf{u}, \mathbf{v})$ is related to the detector transmission function as follows:

The transmission function is specified as a function of proton (or electron) speed, direction of incidence relative to the detector, and the quantity u giving the energy per charge window (see Section 12.2.5.1); it can thus be written as the function $H(\mathbf{v}', u)$, where $\mathbf{v}'$ is the particle velocity vector expressed in a coordinate system Σ' fixed with respect to the detector. If $\mathbf{v}$ is the velocity vector expressed in some suitable coordinate system Σ fixed in space (i.e., not rotating with the spacecraft) and the detector orientation with respect to Σ is given by the direction of $\mathbf{u}$, then

$$G(\mathbf{u}, \mathbf{v}) \equiv H(\mathbf{R} \cdot \mathbf{v}, u) \tag{12.3.3}$$

where $\mathbf{R}$ is the rotation matrix that transforms a vector from Σ to Σ'; clearly $\mathbf{R}$ depends on the angles θ, ϕ specifying the direction of $\mathbf{u}$, and on the angle ψ if relevant (see Section 12.2.5.1). If the width of the transmission function in energy is proportional to the energy, i.e., the quantity $\Delta E/E$ discussed in Section 12.2.2 is independent of E (this is the case for most curved-plate analyzers and for Faraday cups in which the ratio of ac to dc components of the modulating voltage is constant), then $G(\mathbf{u}, \mathbf{v})$ depends only on the directions of $\mathbf{u}$, $\mathbf{v}$ and on the ratio of the magnitudes u/v; thus it can be written as

$$G(\mathbf{u}, \mathbf{v}) = G^*(\mathbf{u}/u, \mathbf{v}/u) \tag{12.3.4}$$

If the detector does not count individual particles but measures currents, the contribution of each species is weighted by its charge and Eq. (12.3.2) is replaced by the following equation for the current $I(\mathbf{u})$:

$$I(\mathbf{u}) = eS \sum_a Z_a \int d\mathbf{v}\, v_n G(\mathbf{u}(Z_a/A_a)^{1/2}, \mathbf{v}) f_a(\mathbf{v}) \tag{12.3.5}$$

The velocity distribution function is also a function of space and time; hence, if the measurement is made at a time t while the spacecraft is located at position $\mathbf{r}$, strictly speaking $f(\mathbf{v})$ in the above equations should be written as:

$$(1/\tau) \int_t^{t+\tau} dt'\, f(\mathbf{r}, \mathbf{v}, t'), \tag{12.3.3}$$

where τ is the duration of the measurement (the change in $\mathbf{r}$ during an interval τ is, in practice, negligible). For the type of detailed analysis described later in this section to be meaningful, it is necessary that the distribution function not change significantly during the time required for the acquisition of one complete set of measurements; as described earlier, for present instruments this time is of the order of minutes. If the plasma changes appreciably on shorter time scales, the time and velocity dependences of the distribution function cannot be distinguished. (If, however, the changes are all random fluctuations on a time scale much shorter than

the duration τ of a single measurement, e.g., high frequency plasma waves, then the analysis is again meaningful but it now yields information only on the distribution function averaged over the fluctuations.)

The contributions to the measurements of different ion species can be separated in principle only by using a suitable instrument, such as the velocity selector. In practice, the predominant positive component of extraterrestrial plasma is protons with a small admixture of alpha particles (approximately 4–10% by number in the solar wind).[1] As can be seen from Eqs. (12.3.2) and (12.3.5), alpha particles are detected at voltages which are twice those for protons, for the same velocity distribution functions. In the solar wind both distribution functions are narrow and the proton and alpha contributions appear as two well-separated peaks in the energy per charge spectrum; thus the two species can be distinguished even without special instruments. To simplify the following discussion, we shall treat the plasma as consisting only of protons and electrons; extensions to other species are straightforward.

Instead of the current $I(\mathbf{u})$ or counting rate $C(\mathbf{u})$ it is convenient to deal with an equivalent quantity having the dimensions of a flux density, $F(\mathbf{u})$, defined as

$$F(\mathbf{u}) \equiv C(\mathbf{u})/S \quad \text{or} \quad F(\mathbf{u}) \equiv I(\mathbf{u})/eS,$$

which is sometimes loosely referred to as "the measured flux." Equations (12.3.2) and (12.3.5) then both become (considering only one species)

$$F(\mathbf{u}) = \int d\mathbf{v}\, v_n G(\mathbf{u}, \mathbf{v}) f(\mathbf{v}). \tag{12.3.6}$$

The basic unfolding problem of extraterrestrial plasma measurements then is: given the measured values $F(\mathbf{u})$ at a discrete set of $\mathbf{u}$, what information can be obtained about the distribution function $f(\mathbf{v})$?

If $F(\mathbf{u})$ were known for all values of $\mathbf{u}$ (considered as a continuous variable), then Eq. (12.3.6) would be a three-dimensional integral equation for $f(\mathbf{v})$; it can be shown, for the special case of a detector whose response is axially symmetric and of the form given by Eq. (12.3.4), that the integral equation (12.3.6) can be explicitly inverted by expanding all functions in spherical harmonics and taking Mellin transforms in energy. This explicit inversion, however, appears to be of no practical use whatever, and approximate methods must be used to solve the unfolding problem.

12.3.2.1. Differential and Integral Behavior. There are two limiting cases in which Eq. (12.3.6) assumes a much simpler form. The first occurs when the distribution function has a much greater width in velocity space than the transmission function and $f(\mathbf{v})$ in (12.3.6) does not vary appreciably

over the range of $\mathbf{v}$ for which $G(\mathbf{u}, \mathbf{v})$ is different from zero; then $f(\mathbf{v}) \approx f(\mathbf{u})$ can be taken out of the integral and (12.3.6) rewritten as

$$F(\mathbf{u}) = [f(\mathbf{u})u^2/m]mu^2\xi,$$
$$\xi \equiv u^{-4} \int d\mathbf{v}\, v_n G(\mathbf{u}, \mathbf{v}). \tag{12.3.7}$$

The quantity in brackets will be recognized as the flux density per unit energy of particles with velocity $\mathbf{u}$, i.e., the differential directional intensity familiar in radiation belt studies. ξ is dimensionless and, if G can be written in the form (12.3.4), depends only on the direction and not the magnitude of $\mathbf{u}$; $u^3\xi$ can be thought of as the effective volume of the transmission function in velocity space.* (Note, however, that $u^3\xi$ in general *cannot* be written in the at first sight "obvious" manner as $\Delta v_n\, \Delta v_{t1}\, \Delta v_{t2}$, where Δv_n and Δv_{t1}, Δv_{t2} are the ranges of velocity along the normal and the two transverse directions accepted by the detector, or in the equivalent polar coordinate form $u^2\, \Delta v_n\, \Delta\theta\, \Delta\phi$, since the range of acceptance in one velocity component may strongly depend on the other components, as illustrated in Fig. 7.) Thus in this limiting case the "measured flux" $F(\mathbf{u})$ is proportional to the differential flux at the point in velocity space corresponding to the center of the detector energy window and angular orientation, with a constant of proportionality closely related to the width of the transmission function. Measurement of $F(\mathbf{u})$ as a function of $\mathbf{u}$ thus directly yields the distribution function.

The other limiting case occurs in the opposite extreme, when the distribution function is very narrow in comparison with the transmission function; this ordinarily requires that the spread of particle velocities about the bulk velocity of the plasma be very small compared to the bulk velocity itself. In this case an appreciable measured flux is obtained only if the plasma bulk velocity $\mathbf{V}$ lies within the detector energy-angle window, and then $G(\mathbf{u}, \mathbf{v})$ may be assumed not to vary significantly over the range of $\mathbf{v}$ for which $f(\mathbf{v})$ is appreciably different from zero, so that $G(\mathbf{u}, \mathbf{v}) \approx G(\mathbf{u}, \mathbf{V})$ may be taken out of the integral in (12.3.6):

$$F(\mathbf{u}) \approx G(\mathbf{u}, \mathbf{V}) \int d\mathbf{v}\, v_n f(\mathbf{v}) = G(\mathbf{u}, \mathbf{V})nV_n \tag{12.3.8}$$

where n is the number density of the particle species being observed and V_n is the component of $\mathbf{V}$ normal to the entrance aperture [cf. Eq. (12.3.1)]. Thus the "measured flux" $F(\mathbf{u})$ is now proportional to the total flux of

[36] G. C. Theodoridis and F. R. Paolini, *Rev. Sci. Instrum.* **40**, 621 (1969).

* For an extensive description of ξ for curved-plate analyzers, see Theodoridis and Paolini[36] and references therein.

particles; the constant of proportionality is independent of the *width* of the transmission function and depends only on its value at the energy and direction corresponding to the bulk velocity of the plasma. Measurement of $F(\mathbf{u})$ as a function of $\mathbf{u}$ thus serves to fix $\mathbf{V}$ (most easily obtained as the value of $\mathbf{u}$ for which the largest value of F occurs) but provides no information on the shape of the distribution function; the shape of $F(\mathbf{u})$ simply reflects the transmission function.

The first limiting case, in which the detector provides differential measurements of the flux in velocity space, is generally encountered in the outer magnetosphere. The second limiting case, in which the detector provides a measurement of the total integrated flux, is a first approximation to the behavior of all detectors (except those with extremely narrow transmission functions) in the solar wind. In the magnetosheath generally (and for some detectors in the solar wind), the distribution function and the transmission function have comparable widths and the full integral in Eq. (12.3.6) must be retained.

It should also be noted that many detectors have transmission functions which are narrow in one direction and wide in another. For example, hemispherical curved-plate analyzers generally have a very narrow response in energy (approximately a few percent) and azimuthal angle (approximately a few degrees) but a very wide response in polar angle (nearly 90°); a modulated Faraday cup may select particles in a very narrow range of velocity normal to its aperture but accept a wide range of transverse velocities. A more complex case occurs with the quadrispherical analyzer, whose transmission function has a nonzero value over a region of velocity space that is greatly elongated along a direction approximately 70° from normal incidence (see Fig. 7). If the width of the transmission function along its "wide" and along its "narrow" direction is much larger and much smaller, respectively, than the width of the distribution function, the "measured flux" $F(\mathbf{u})$ is proportional to the flux integrated over the "wide" direction but differential along the "narrow" direction. As a function of $\mathbf{u}$, $F(\mathbf{u})$ then has a hybrid character: its dependence on the component of $\mathbf{u}$ along a "narrow" direction reflects the behavior of $f(\mathbf{v})$, while its dependence on the component of $\mathbf{u}$ along a "wide" direction simply reproduces the transmission function. If the existence of these different widths in the transmission function is not appreciated, the resulting behavior of $F(\mathbf{u})$ may be falsely attributed to an anisotropy in the distribution function.*

[37] A. J. Hundhausen, *J. Geophys. Res.* **74,** 3740 (1969).

* Compare the discussion of Pioneer 6 measurements by Hundhausen.[37]

12.3.3. Estimation of Plasma Parameters

12.3.3.1. Method of Moments. As discussed above, most of the effort in data analysis, particularly in the case of the solar wind, has gone into estimating the hydrodynamic parameters of the plasma (moments of the distribution function). The simplest method for estimating these is obtained if one assumes that the detector can, to some approximation, be treated as differential; then, if the measurements are made at energies and angles specified by $\mathbf{u}_j$ $(j = 1, 2, \ldots, N)$, each measurement provides a value of the distribution function $f(\mathbf{v})$ according to Eq. (12.3.7). Now a particular moment M_p of $f(\mathbf{v})$ can be approximated by a sum

$$M_p \equiv \int d\mathbf{v}\, \mathbf{v}^p f(\mathbf{v}) \approx \sum_{j=1}^{N} C_j \mathbf{u}_j{}^p f(\mathbf{u}_j),$$

where the C_j are constants obtained from the usual theory of approximate numerical quadrature; substituting for $f(\mathbf{u}_j)$ from Eq. (12.3.7), we obtain an estimate of the moment M_p as a linear combination of the measured fluxes:

$$\begin{aligned} M_p &\approx \sum_{j=1}^{N} \alpha_i^{(p)} F(\mathbf{u}_j), \\ \alpha_j^{(p)} &\equiv C_j \mathbf{u}_j{}^p / u_j{}^4 \xi. \end{aligned} \tag{12.3.9}$$

This method has been extensively used to analyze measurements in the outer magnetosphere, where the assumption of differential detector behavior is usually well justified. It has also been used with some success to obtain the proton density and bulk velocity (but not pressure) from measurements in the solar wind.[38,39] As the assumption of differential behavior is in this case clearly inappropriate, the justification of the method is purely empirical and the coefficients $\alpha_j^{(p)}$ in Eq. (12.3.9) are obtained empirically by requiring the method to yield the correct results when applied to a set of $F(\mathbf{u}_i)$ calculated (using Eq. (12.3.8)) from a model distribution of known density and bulk velocity; in this case the extreme computational speed of the method of moments is its sole advantage over the method described in the following section.

12.3.3.2. Use of Model Distributions. By far the most extensively used method has been to assume a specific functional form of the distribution function containing some adjustable parameters, calculate the expected

[38] E. F. Lyon, A study of the interplanetary plasma. Ph.D. Thesis, M.I.T., Cambridge, Massachusetts, 1966 (unpublished).

[39] A. J. Lazarus, H. S. Bridge, J. M. Davis, and C. W. Snyder, *Space Res.* **7,** 1296 (1967).

fluxes from Eq. (12.3.8) as functions of the parameters, and then vary the parameters until the predicted and the measured fluxes agree as closely as possible. (The adjustable parameters very often are the moments of the distribution themselves.) While this method is not expected to yield precise information on the detailed shape of $f(\mathbf{v})$, the estimated moments of the distribution function should be relatively accurate provided that its actual shape does not greatly differ from the assumed model and that a significant fraction of the particles lies within the region of velocity space surveyed by the detector. For the use of this method to be meaningful it is, of course, necessary that there be more measurements than adjustable parameters to be fitted to them.

Various methods of fitting have been used. The classical least-squares technique is the most straightforward, although rather cumbersome and time-consuming. Simplified methods, generally tailored to the specific characteristics of a particular set of observations, have been evolved[15,17,40]; most of them estimate the parameters from a few selected measurements and use the remaining measurements to verify and/or improve these estimates.

Among the principal model distributions used to date are the following:

(1) Convected Maxwellian:

$$f(\mathbf{v}) = \frac{n}{\pi^{3/2} w_0^{\,3}} \exp\left\{ - \frac{(\mathbf{v} - \mathbf{V})^2}{w_0^{\,2}} \right\}.$$

Adjustable parameters are: density n, bulk velocity $\mathbf{V}$, and most probable speed w_0 (related to temperature T by $kT = \frac{1}{2} m w_0^{\,2}$). This is the simplest model and the first one used.[41] When used to fit solar wind data from detectors whose transmission functions are much wider than the proton distribution function, it yields good values of the density and bulk velocity (more accurate than those obtained by the method of moments) plus a rough estimate of the width of the distribution function.

(2) Convected bi-Maxwellian[24,42,43]:

$$f(\mathbf{v}) = \frac{n}{\pi^{3/2} w_{0\parallel} w_{0\perp}^{\,2}} \exp\left\{ - \frac{w_\parallel^{\,2}}{w_{0\parallel}^{\,2}} - \frac{w_\perp^{\,2}}{w_{0\perp}^{\,2}} \right\},$$

$$\mathbf{w} \equiv \mathbf{v} - \mathbf{V}, \qquad w_\parallel = \mathbf{w} \cdot \mathbf{b}, \qquad \mathbf{w}_\perp = \mathbf{w} - \mathbf{b} w_\parallel .$$

[40] M. Neugebauer and C. W. Snyder, *J. Geophys. Res.* **71,** 4469 (1966).
[41] F. Scherb, *Space Res.* **4,** 797 (1964).
[42] F. L. Scarf, J. H. Wolfe, and R. W. Silva, *J. Geophys. Res.* **72,** 993 (1967).
[43] V. Formisano, *J. Geophys. Res.* **74,** 355 (1969).

Adjustable parameters are: density n, bulk velocity $\mathbf{V}$, and parallel and perpendicular thermal speeds $w_{0\parallel}$ and $w_{0\perp}$; $\mathbf{b}$ is the unit vector along the magnetic field and is generally known from simultaneous measurements on the same spacecraft. This appears to be, at present, a reasonably close approximation to the actual proton distribution function in the solar wind.

(3) The function

$$f(\mathbf{v}) = \frac{n}{\pi^{3/2} w_0{}^3} \frac{\Gamma(\kappa + 1)}{\kappa^{3/2}\Gamma(\kappa - \frac{1}{2})} \left[1 + \frac{|\mathbf{v} - \mathbf{V}|^2}{\kappa w_0{}^2}\right]^{-(\kappa+1)}$$

which is a generalization of the "resonance" distributions used in plasma physics (the case $\kappa = 2$ is also known as the Cauchy distribution) and is sometimes known in the trade as the "κ-distribution." The adjustable parameters are the density n, the bulk velocity $\mathbf{V}$, the most probable speed w_0, and the exponent κ; at large values of v ($|\mathbf{v} - \mathbf{V}|^2 \gg w_0{}^2$) the distribution function varies approximately as (energy)$^{-\kappa-\frac{1}{2}}$ [the corresponding differential intensity varies as (energy)$^{-\kappa}$]. As $\kappa \to \infty$, $f(\mathbf{v})$ approaches the Maxwellian distribution. This function has been used mainly to analyze measurements of electrons in the magnetosheath and the outer magnetosphere (in the latter case the bulk velocity is usually assumed *a priori* to be negligible), in order to represent the effects of a large non-Maxwellian high-energy "tail" that appears to be present in the electron distribution function within these regions.[14,17,44]

As an example of the use of this method, Fig. 9 shows two sets of Faraday cup measurements on the IMP-1 satellite, together with theoretically calculated fluxes from the fitted models.

12.3.3.3. Construction of the Distribution Function by Interpolation. As already pointed out in Section 12.3.2, if the distribution function is very wide compared to the transmission function, the measured flux $F(\mathbf{u})$ directly gives the distribution function. If the widths of the transmission function and the distribution function are comparable, it may still be possible to bypass model construction and obtain the distribution function at a particular point by interpolating between several measured fluxes. Techniques for doing this have been developed by Hundhausen *et al.*[45] and by Ogilvie *et al.*[46] In essence, one considers a few adjacent measure-

[44] A. J. Lazarus, G. L. Siscoe, and N. F. Ness, *J. Geophys. Res.* **73,** 2399 (1968).

[45] A. J. Hundhausen, J. R. Asbridge, S. J. Bame, H. E. Gilbert, and I. B. Strong, *J. Geophys. Res.* **72,** 87 (1967).

[46] K. W. Ogilvie, L. F. Burlaga, and H. Richardson, Goddard Space Flight Center Rep. X-612-67-543. Goddard Space Flight Center, Greenbelt, Maryland, 1967.

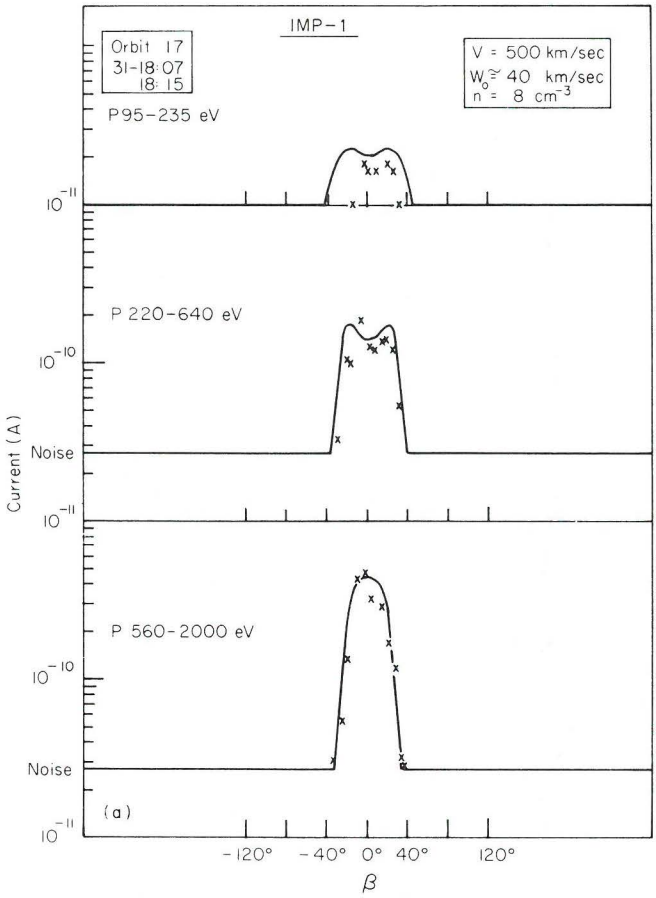

FIG. 9. A set of Faraday cup measurements on IMP-1 and model distributions fitted to them. Shown are currents measured in each energy window as a function of spacecraft rotation angle β; + and × are measured values, lines are theoretical fits. Above: Proton measurements in the solar wind. A convected Maxwellian has been assumed. Right: Measurements in the magnetosheath. The "contamination" of proton measurements by electrons (see Section 12.2.2.1) is in this case significant. A convected Maxwellian has been assumed for protons and a κ-distribution for electrons. Dashed lines: predicted currents due to protons alone. Solid lines: predicted currents due to protons and electrons [from S. Olbert, *in* "Physics of the Magnetosphere" (R. L. Carovillano, J. F. McClay, and H. R. Radoski, eds.), p. 641. Reidel, Dordrecht, Holland, 1969].

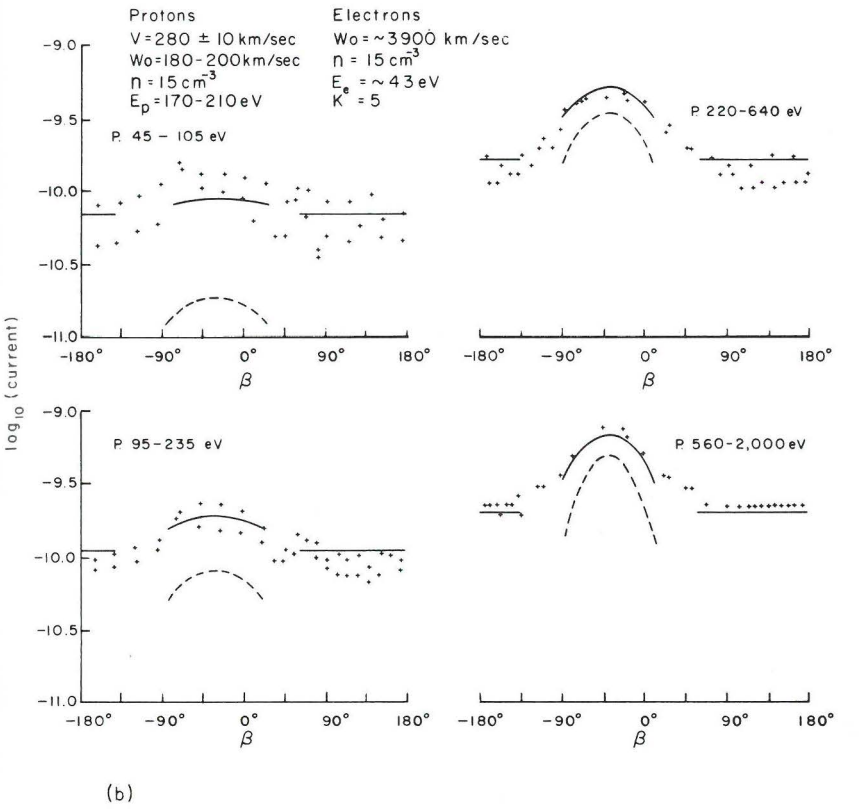

FIG. 9.

ments at a time [for example $F(\mathbf{u})$ for $\mathbf{u}_{j-1}$, $\mathbf{u}_j$, $\mathbf{u}_{j+1}$] and assumes that both the function $F(\mathbf{u})$ for $\mathbf{u}$ near $\mathbf{u}_j$ and the distribution function $f(\mathbf{v})$ for some narrow range of $\mathbf{v}$ about $\mathbf{v} = \mathbf{u}_j$ can be represented by Gaussian functions (the transmission function is also usually approximated by a Gaussian or by a step function); then it is possible to solve for the value of $f(\mathbf{v})$ at $\mathbf{v} = \mathbf{u}_j$ in terms of the adjacent measured values $F(\mathbf{u})$ for $\mathbf{u} = \mathbf{u}_{j-1}$, $\mathbf{u}_j$, $\mathbf{u}_{j+1}$. By taking a series of adjacent groups of measurements, values of $f(\mathbf{v})$ at a series of $\mathbf{v} = \mathbf{u}_j$ for all j can be obtained; values of $f(\mathbf{v})$ at intermediate values of $\mathbf{v}$ can then be obtained by conventional

interpolation, and moments of $f(\mathbf{v})$ can be calculated, if desired, by numerical integration over the function thus obtained. An example of a solar wind proton distribution function constructed in this manner from curved-plate analyzer measurements on the Vela 3 satellite is shown in Fig. 10.*

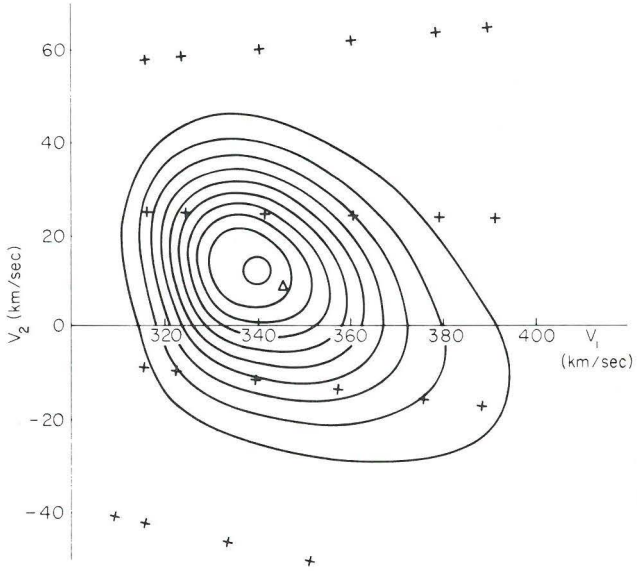

FIG. 10. Contour map of a proton velocity distribution function in the solar wind obtained from a set of Vela 3 curved-plate analyzer measurements. The function is normalized to a maximum value of 1 and the contours are drawn at intervals of $\frac{1}{10}$. The triangle shows the bulk velocity. The $\times$'s indicate the the points $\mathbf{u}_j$ at which the actual measurements were made; the width of the transmission function along the V_1 or V_2 direction is comparable to the spacing of the $+$'s along that direction [from A. J. Hundhausen, J. R. Asbridge, S. J. Bame, H. E. Gilbert, and I. B. Strong, *J. Geophys. Res.* **72,** 87 (1967)].

* ACKNOWLEDGMENTS: I am grateful to Professors H. S. Bridge, S. Olbert, and A. J. Lazarus for critical reading of the manuscript. This work was supported by the National Aeronautics and Space Administration under grant NGL 22-009-015.